A new ultrasonic technique for detection and location of defects in three-layer plastic pipes with a reinforced internal layer

R. Kažys, O. Tumšys, D. Pagodinas

Prof. K.Baršauskas Ultrasound Institute,
Kaunas University of Technology,
51328 Kaunas, Lithuania

Abstract

Ultrasonic non-destructive testing (NDT) of the multi-layer and fibre-reinforced composites meets some specific problems caused by a high acoustic attenuation and a high structure noise due to scattering of ultrasonic waves by fibre-reinforced layer and due to multiple reflections inside the samples caused by different acoustic impedances of the layers.

Objective of this study was to develop the new signal processing technique for detection of defects in three-layer plastic pipe with internal fibre-reinforced layer. The proposed method consists of the improved algorithm eliminating the signals reflected by interfaces of the pipe layers, the optimized mother wavelet analysis and manipulation by the wavelet coefficients. The elimination of the reflected signals by interfaces is based on subtracting from each analyzed signal the reference signal. Further the processed signal is decomposed into a sum of elementary wavelets. The optimal mother wavelet is chosen according to the introduced weighting coefficients and results of investigations of echo signals, reflected by different artificial defects in a multi-layer plastic pipe.

Keywords: three-layer plastic pipe, ultrasonic NDT, signal processing, wavelet transform.

1. Introduction

Ultrasonic non-destructive testing (NDT) methods are widely used for testing of various synthetic products [1, 2]. For example, ultrasound has found numerous applications in characterization of various polymers [3-5]. A novel problem arising in this field is non-destructive testing and evaluation of multi-layer plastic pipes with fibre-reinforced layer. The purpose of such a testing is detection and sizing of various defects, which are arising during manufacturing process.

Detection of defects using ultrasonic techniques involves many factors, which influence the transmitted ultrasonic signal in the material under investigation. NDT of the multi-layer and fibre-reinforced composites meets some specific problems caused by a high acoustic attenuation and a high structure noise due to scattering of ultrasonic waves by fibre-reinforced layer and due to multiple reflections inside the samples caused by different acoustic impedances of the layers. Attenuation of ultrasonic waves is due to absorption and scattering phenomena [1]. The absorption converts acoustic energy into heat via viscosity, relaxation, heat conduction, elastic hysteresis, etc. The absorbed energy of the acoustic field is irreversibly lost since it is dissipated in the medium. The absorption is essentially independent of particle size, shape and volume.

Scattering converts the energy of the coherent, collimated beam into incoherent, divergent waves. This is result of wave interaction with non-uniformities in the material. The scattering by micro structural components of a material causes serious difficulties in detection of discontinuities, as it reduces the signal to noise ratio (SNR). The scattering from boundaries between small, randomly distributed particles in the materials create small ripples in the reflected ultrasonic signals, which in NDT are referred to as a structure noise. The ultrasonic structure noise is time invariant and correlated with the useful signal. This noise limits detection of small cracks, pores or other discontinuities.

The named problems show that testing of multi-layer materials requires a special care in frequency selection and signal interpretation. Many investigators have studied the detection of defects in multi-layer inhomogeneous structures using analytical, experimental or computational approaches [6-9]. The ultrasonic wave propagation and interaction in such structures is a complex issue. The signal received by the transducer can be described by the ray tracing, transfer matrix or hybrid method [10]. Wave propagation and scattering in inhomogeneous materials can be modelled using the finite element method, the boundary element method or 3D elastodynamic model [11, 12]. The internal defects in composite materials can be detected by using different signal processing algorithms [13-15]. All of these researches must be improved detection and location of defects in multi-layer materials.

The objective of the present research is to develop the new signal processing technique for detection of defects in three-layer plastic pipe with internal fibre-reinforced layer (Fig.1). Short pulses of ultrasound have been employed for layer-by-layer imaging of internal structure of the pipe. The structure image strongly depends on the layers microstructure and their mechanical properties. The microstructure of the internal layer of the pipe is associated with proportion and orientation of fibers, fiber arrangement, homogeneities of material components, interfaces, micro-defect, etc. In this paper, we proposed the new ultrasonic signal processing technique with reference of the experimental investigations of this plastic pipe sample. Reliable detection and characterization of defects in this structure may be improved by applying signal processing of the received ultrasonic signals. The used digital signal-processing algorithm is based on the Discrete Wavelet Transform (DWT). The performance of the proposed algorithm was estimated analyzing measurement errors of the size and location of the artificial defects in the internal glass fibre-reinforced layer.

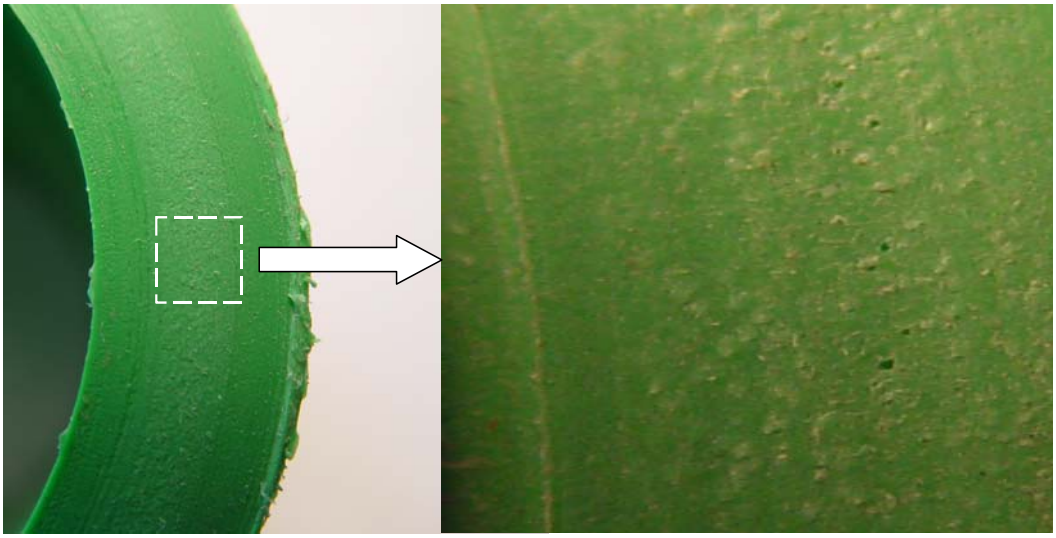

a b

Fig.1. **View of the three-layer plastic pipe sample (a) with internal fibre-reinforced layer (b).**

2. Experimental investigation

The ultrasonic-based inspection system of the defects detection is based on a pulse-echo immersion technique. The ultrasonic wave, generated by a piezoelectric transducer propagates through each layer of the three-layer pipe and is reflected by all discontinuities of the layers, including front and back surfaces of the layers (Fig.2.). This wave travels through the inhomogeneous structure of the second glass-fibre reinforced layer and in this layer changes the shape and spectral content.

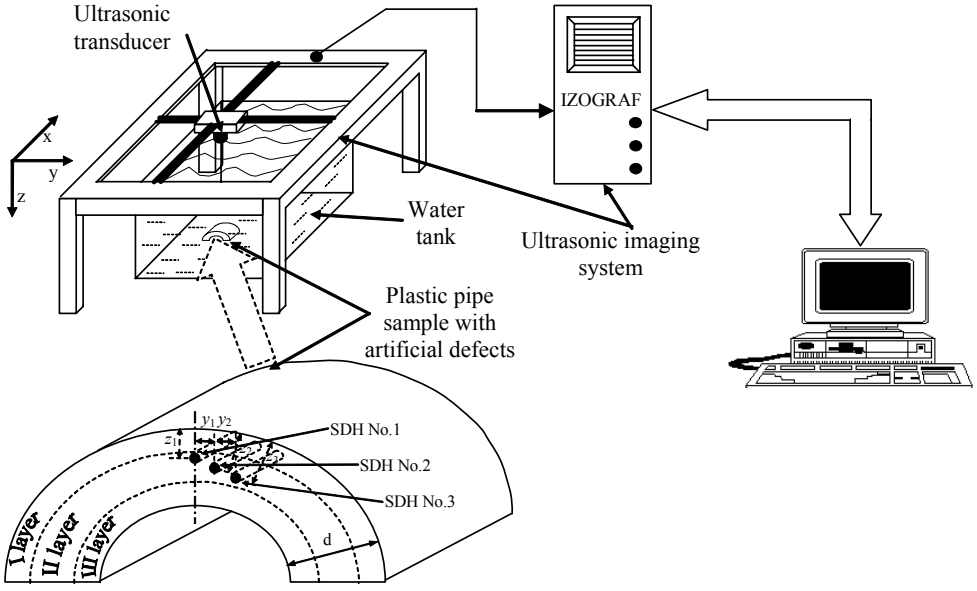

Fig.2. **Experimental set-up for investigation of the three-layer plastic pipe using the ultrasonic NDT system "Izograf"**

The experimental investigation was carried out using the imaging system "Izograf", developed in Ultrasound institute of the Kaunas University of Technology. As an ultrasonic transmitting/receiving transducer the Panametrics transducer V308 (the resonance frequency 5 MHz, the aperture 19 mm) was used. The transducer was excited by the 140 V amplitude and 80 ns duration electrical pulse. This transducer is spherical in shape and is focused at the distance of 48 mm from the centre of the emitting surface. The reflected signals are presented on the graphical screen in the form of *A-scans* and *B-scans*.

Experimental ultrasonic investigations of fibre-reinforced composites were carried out using a three-layer plastic pipe sample [16]. All three layers were of polypropylene; the internal layer was with the fibre glass infusion. The wall thickness of this pipe sample was d=10.8 mm, the thickness of the layers were the following: d_1=3.0 mm, d_2=3.8 mm, d_3=4.0 mm. In the pipe sample

artificial defects – side-drilled holes (SDH) – at known position were drilled. The distances of the holes from the front surfaces were z_1=5.0 mm, z_2=5.9 mm, z_3=6.7 mm respectively. The distance between the holes SDH No.1 and No.2 was y_1=3.0 mm, between the holes SDH No.2 and 3 was y_2=2.5 mm. The lengths of the side drilled holes were the following: x_1=6.3 mm, x_2=5.1 mm, x_3=4.4 mm. The diameter of all holes was 0.7 mm.

For detection of the artificial defects in the internal layer of sample we have used *A*- and *B-scans* obtained by scanning of the transducer along the coordinate *x*. The example of the *B-scan* along the artificial defect SDH No.1 is presented in Fig.3c. In Fig.3a and b *A-scans* at the fixed point of this *B-scan* with and without artificial defect are presented. In this figure we have translated the measured time of flight (TOF) t_i of the each *A-scan* in the *B-scans* into the spatial coordinate $z_i(t)$ according to the formula:

$$z_i(t) = c_{aver.}\left(\frac{t_i}{2} - \frac{l_w}{c_w}\right), \qquad (1)$$

where c_{aver} is the averaged ultrasound velocity in a three-layer plastic pipe sample; l_w is the distance between the transducer and the front surface of the sample and c_w is the ultrasound velocity in water. This translation we have introduced in order to compare the real wall thickness *d* of the plastic pipe and the actual defect positions along the coordinate *z* with the measured ones by the proposed ultrasonic method.

The averaged ultrasound velocity was calculated according to the ultrasound velocities c_1, c_2 and c_3 measured in the layers I, II and III respectively:

$$c_{aver.} = \frac{2d}{\frac{2d_1}{c_1} + \frac{2d_2}{c_2} + \frac{2d_3}{c_3}} = \frac{dc_1c_2c_3}{d_1c_2c_3 + d_2c_1c_3 + d_3c_1c_2}. \qquad (2)$$

The measurements results of ultrasound velocities are the following: c_1=2500 m/s; c_2=2240 m/s; c_3=2400 m/s. The calculated averaged ultrasound velocity for the analyzed plastic pipe is $c_{aver.}$=2367 m/s.

The *A*- and *B-scans* presented in Fig.3 shows the problems to detect of the defects in the inhomogeneous internal layer of the three-layer plastic pipe sample. How it is seen from Fig.3c the echoes in the three-layer pipe sample with the artificial defect SDH No.1 consist of the multiple reflections caused by the front surfaces of I and II layers and the back surface of the pipe wall. The front surface of the layer III is not detected. This is caused by the high attenuation of the plastic pipe and by comparable acoustic impedances of the layers.

The second problem is caused by the signals, reflected by the front surface of the plastic pipe sample. On can see in the collected *B-scan* that these signals are also noticeably distorted due to a limited dynamic range of the instrumentation (Fig.3a and b). These signals with a large amplitude complicate processing of the signals with small amplitude in the second layer. For reducing influence of these signals we have applied the time window (Fig.3c dashed line) to eliminate the signals reflected by the front surface of the pipe and to improve the SNR. The *B-scan* obtained after such procedure is shown in Fig.3d.

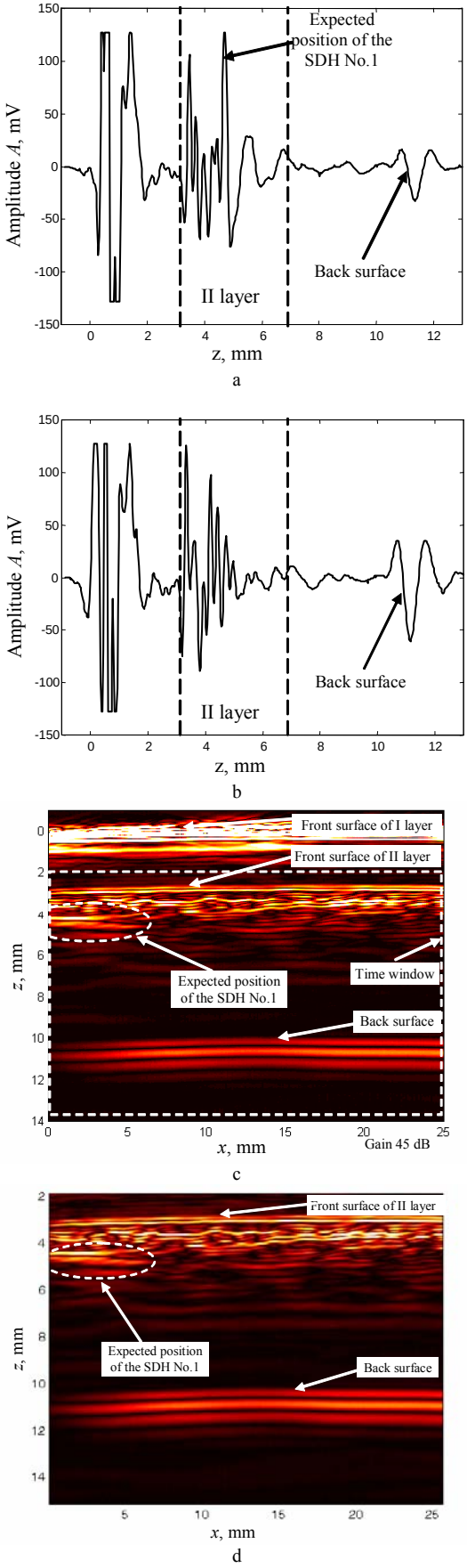

Fig.3. ***A-scans* at fixed points of *B-scans* collected along coordinate *x* with the artificial defect SDH Nr.1 with (a) and without (b) artificial defect, and collected *B-scan* (c) and time windowed *B-scan* (d).**

The biggest problem is complication of the detection of the defects due to a structure noise caused by scattering of ultrasonic waves by the fibres. This noise is time invariant and slightly correlated with the echoes from defects. Therefore, the defect SDH No.1 in the layer II cannot be detected reliably also. The signals reflected by the fibres can be seen clearly in the *B-scan* (Fig.3c, d depth z=(3-5) mm). For reduction of this structure noise we have proposed the new signal processing algorithm based on the wavelet transform method.

3. Signal processing

The structure noise is uniformly distributed in the time-frequency domain. Several specific methods have been proposed for the reduction of this type of noise based on time-frequency distribution of the analysing signals [17-21].

The discrete wavelet transform is a well established technique for removing noise from signals [18-21]. This method decomposes the ultrasonic signal into a sum of elementary contributions called wavelets [22]. The wavelet coefficients in the time-frequency domain represent the signal and the noise. Manipulation by the wavelet coefficients enables reduce influence of noise and is based on a coefficient shrinking. The most extensively used technique is the soft or hard threshold method [23-25]. Using this approach, all wavelet coefficients whose modulus is smaller than the threshold are discarded, and the remainder values are used to reconstruct the signal. The inverse wavelet transform is used to reconstruct the de-noised signal. This approach is optimal for white noise, but it can fail if the noise is correlated, as in our case.

Wavelet threshold estimators for data with stationary correlated noise are constructed by applying level-dependent thresholds (using the universal threshold and the soft thresholding rule) to the coefficients in the wavelet transform [26].

Our investigation has shown that direct application of the wavelet level-dependent thresholding in the analysed case meets rather essential problems which reduce its efficiency. Ultrasonic signals reflected by the front surface of the pipe are significantly stronger than the signals reflected by internal discontinuities; therefore if the gain of the instrumentation is selected in order to reveal weaker signals, then the signal reflected by the front surface is non-linearly distorted. The signals reflected by the surface of the layer II and artificial defects are comparable by the amplitude, therefore the defects may be drown in the tail of this signal and the structure noise. Efficiency of the wavelet transform (WT) is reduced by these stronger signals which actually do not possess any information about flaws in the internal layer. Therefore we propose to select from the collected B-scans only the signals from the fibre-reinforced layer and in this way to improve performance of the signal processing by the WT. To carry out this selection automatically is not a trivial task due to a few reasons. This selection should be carried out or along the pipe, or across depending on a scanning direction. The surface of the pipe in a general case is not parallel to the scanning path. The position of the signal reflected by the interface between the first and the second layers in the space - time domain is random due random distribution of the fibres. It means that simple selection of the necessary part of the signal by the time window is not feasible. The proposed algorithm consists of the following steps:

- elimination of the spatial trend in the collected B-scans;
- reduction of the ultrasonic signals reflected by the interface between the external (I) and internal (II) layers;
- decomposition of each selected A-scan type signal into a sum of elementary wavelets;
- shrinking of the wavelet coefficients;
- reconstruction of the signal from the selected wavelet coefficients;
- application of the Hilbert transform and calculation of the spatial-temporal envelope of the B-scan.

The first step in the signal processing is check for a trend in the scanning direction (in our case the coordinate x) of the collected *B-scan* (Fig. 3d). The position of the signal reflected by the front surface of the layer II is not known precisely in advance due to possible curvature of the sample, non-parallelism of the scanning path with respect to the surface of the pipe, random deviations of the surface from a planar case, etc. Therefore in the time domain each *A-scan* possesses a time trend Δt_i with respect to other *A-scans* collected along the coordinate x. This trend may be approximated by a linear function $\Delta t_i = kx_i$, where k is the constant. To compensate this trend we measured the delay time of the echo-signals, reflected by the front surface of the layer II of each *A-scan* at the selected threshold, calculated the time trend Δt_i and shifted each *A-scan* in the time domain by the found trend value Δt_i:

$$s_{tr}(x_i, t) = s(x_i, t - \Delta t_i). \quad (3)$$

The second step is elimination of the ultrasonic signals reflected by the front surface of the layer II and fibres close to it, which may be irregular in a spatial domain. The signals reflected by the front surface of the layer II have high amplitude and mask the useful signal. The signals reflected by the fibres are less than signals reflected by the defect but are randomly distributed and operate as a structural noise. The partially elimination of this useless signals is based on subtracting some reference signal $s_{ref}(t)$ from each *A-scan* signal $s_{tr}(x_i, t)$ in the collected *B-scan* (Fig. 3d):

$$s_e(x_i, t) = s_{tr}(x_i, t) - s_{ref}(t). \quad (4)$$

The reference signal $s_{\text{ref}}(t)$ is obtained by picking-up signals reflected in the region without defects (Fig. 3d). The analysis of reference signals formed in different ways shows that the best results are obtained using the reference signal calculated as an average of at least ten signals collected at different points along x-axis:

$$s_{ref}(t) = \frac{\sum_{k=1}^{10} s_{tr}(x_k, t)}{10}. \quad (5)$$

where $s_{tr}(x_k,t)$ are the signals collected at the selected points in the region without defects: $s_{tr}(x_k, t) = s_{tr}(x_{(p+(k-1)\Delta p)}, t)$, where $s_{tr}(x_p,t)$ is the signal

at the first selected point *p*. For the analysed plastic pipe this step was selected Δp=1 mm.

Application of this procedure enables significantly reduce the signals reflected by the front surface of the layer II and partially by fibres and bottom surface of this layer and consequently improve the SNR (Fig.4a). However, detection of flaws in the inhomogeneous layer II remains complicated.

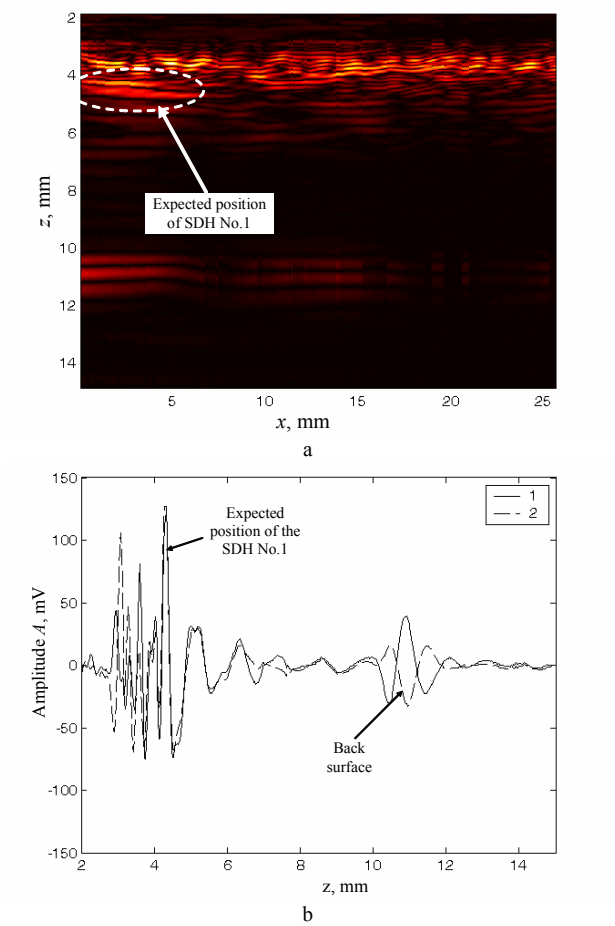

Fig.4. **The *B-scan* of the pipe sample with the artificial defect SDH No.1 processed by the proposed algorithm (a) (*B-scan* before processing is presented in Fig.3d) and the *A-scan* at the fixed point before (b, dashed line) and after signal processing (b, solid line).**

Therefore for improvement of detection and characterization of defects in the inner fibre reinforced layer we propose to apply the discrete wavelet transform. The DWT represents the original *A-scan* signal $s(n)$ in terms of the shifted version of a low-pass scaling function $\varphi(n)$ and shifted and dilated versions of the prototype band pass wavelet function $\psi(n)$ [24]. The low and high-pass wavelet coefficients are defined as:

$$\lambda_{j+1}(k) = \sum_n h(n-2k)\lambda_j(n), \qquad (6)$$

$$\gamma_{j+1}(k) = \sum_n g(n-2k)\lambda_j(n), \qquad (7)$$

where subscript j indicates the scale or the resolution of analysis; k shows the spatial location of analysis; $h(n)$ and $g(n)$ are the impulse responses of a low and high-pass filters respectively. Thus, the original signal can be represented as a finite sum of the coefficients calculated of the shifted and dilated mother wavelets:

$$s(n) = \sum_{j=1}^{J}\sum_k \gamma_{j,k}\psi_{j,k}(n) + \sum_k \lambda_{J,k}\varphi_{J,k}(n), \qquad (8)$$

where J is the maximal decomposition level. The maximal level J of decomposition depends on the length of the signal in terms of samples:

$$J = \log_2 N - 1. \qquad (9)$$

During this step of the signal processing each A-scan with the eliminated time trend and suppressed reflections from the interfaces we decompose into elementary wavelets (Eq.8). Because we use the A-scans with N=512 samples and the signal sampling frequency 50 MHz, the maximal level of the signals decomposition was J=8 (Eq.9) and the highest frequency range which corresponds to the level 1 was (12.5-25) MHz. The second level corresponds to the frequency range subsampled by two, etc.

Primarily for analyzed A-scans with correlated noise we apply level-dependent thresholds with the universal threshold and the soft thresholding rule. But this procedure showed that detection of SDH No.1 in the internal layer is complicated (Fig.5).

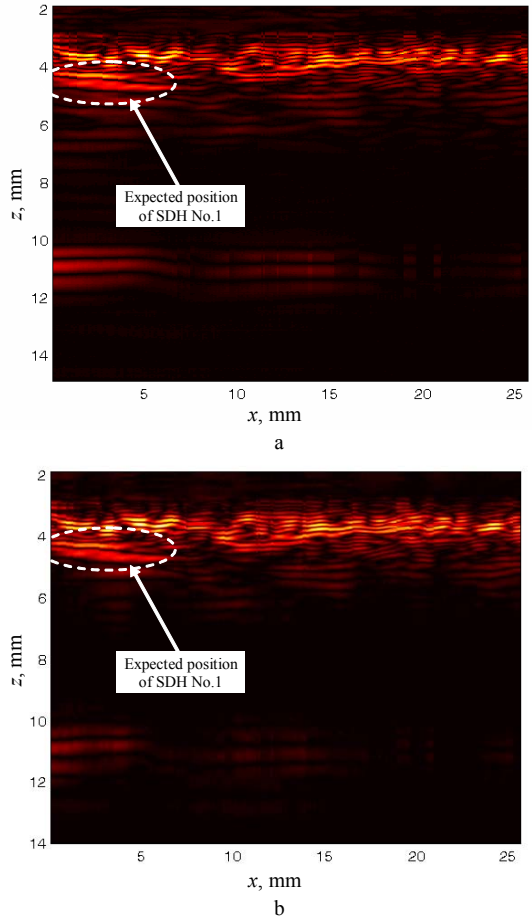

Fig.5. **The *B-scan* of the pipe sample with the artificial defect SDH No.1 after the reduction of the signals reflected by the interfaces (a) and processed by the wavelet level-dependent thresholds using universal threshold and the soft thresholding rule (b).**

Analysis of the *A-scan* signals after the reduction of the signals reflected by the interfaces (Fig. 5a) show that the spectral characteristics of the signals were changed (Fig. 6.). The resonance frequency of the *A-scans* signals without defects was mowed to the low frequencies

(compare to ultrasonic transducer resonance frequency) and was concentrated in 4 and 5 levels band of the wavelet coefficients. However, the spectrum of the *A-scans* signals with artificial defect SDH No.1 has the increasing in the 3 level band of the wavelet coefficient.

To estimate how well the wavelet coefficients of the level j represent the ultrasonic echo-signal from the analysed defect, we propose to use the weighting coefficients [27]:

$$W_j = \frac{\gamma_{j\Sigma}}{\gamma_\Sigma}, \qquad (10)$$

where $\gamma_\Sigma = \sum_{j=1}^{J}\sum_{k}\gamma_{j,k}$; $\gamma_{j\Sigma} = \sum_{k}\gamma_{j,k}$; $\gamma_{j,k}$ are the high pass filter coefficients. Obviously, $\sum_j W_j = 1$.

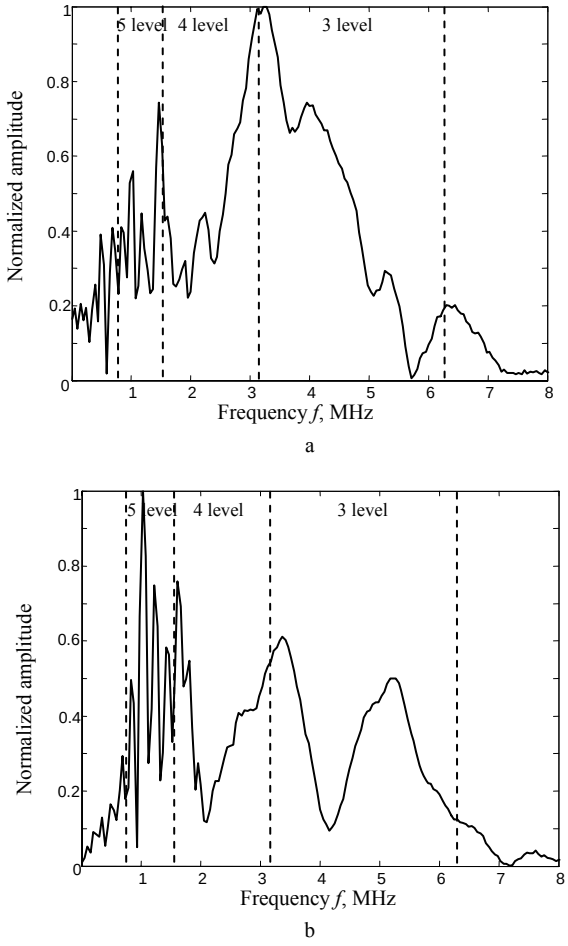

Fig.6. **The processed signals spectrum (magnitude) of the *A-scans* without (a) and with artificial defect SDH No.1 (b) and the bands regions of the levels 3-5 of the wavelet coefficients.**

The analysis of the weighting coefficients (Eq. 10) of the different mother wavelets (Meyer, Haar, Symlet, Coiflet, Daubechies) shows that about 75 % of the wavelet coefficients were concentrated in 3-5 levels. These results are associated with conclusions of defined energy in different levels of the wavelet coefficients of analysed carbon fiber-reinforced composites with acoustic emission signals [28]. Therefore we concentrate to analysis the wavelet coefficients in these levels.

The evaluations of the wavelet coefficients of different artificial defects (Fig. 2, SDH No.1-3) show that the weighting coefficient at the level 5 (0.78-1.56 MHz) best represents these defects. The example of this analysis was presented in Fig. 7. On can see the processed 10 echo signals from the artificial defect SDH No.1 (Fig. 7b) has bigger weighting coefficients at the level 5 (~0.37) compare to 5 level coefficients (~0.12) of the 10 echo signals without defect (Fig. 7a).

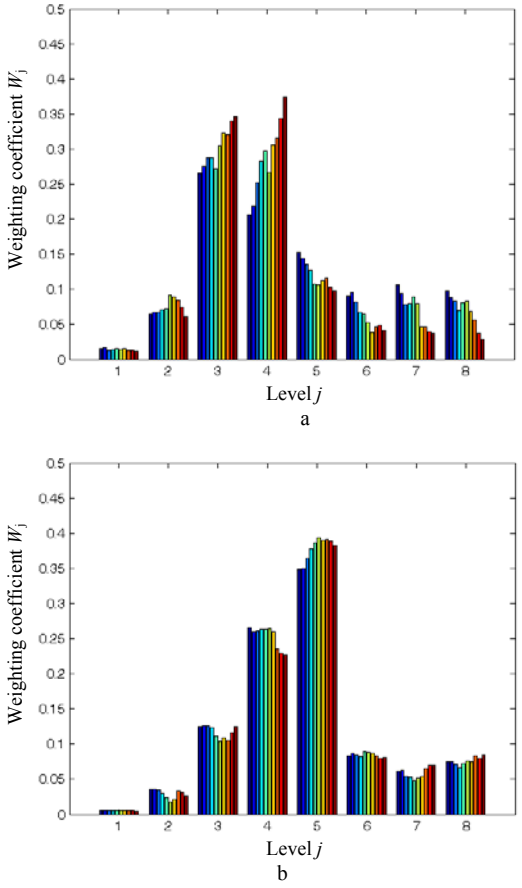

Fig.7. **The weighting coefficients calculated by the "Coiflet-5" wavelet from 10 echo-signals without (a) and with the artificial defect SDH No.1 (b)**

This conclusion we used to determine the optimal mother wavelet for each artificial defect SDH No.1-3. To compare different mother wavelet we propose introduce the difference between the weighting coefficients from each level for different types of defects:

$$\Delta W_j^{di} = W_{jav} - W_{jav}^{di}, \qquad (11)$$

where $W_{jav} = \left(\sum_{k=1}^{10} W_{jk}\right)/10$ and $W_{jav}^{di} = \left(\sum_{k=1}^{10} W_{jk}^{di}\right)/10$ are the averages of the weighting coefficients of 10 samples without and with a corresponding defect, accordingly. The illustration of this difference for side drilled holes is presented in Fig. 8a-c.

As it follows from Fig. 8a-c, the different defects in the inhomogeneous layer II are presented best by the weighting coefficients of the level 5. The optimal mother wavelet was selected such, for which the difference

between the weighting coefficients of the level 5 for different types of defects is the biggest:

$$\psi(n)_{opt} \Rightarrow \max(\Delta W_5^{d1}, \Delta W_5^{d2}, \Delta W_5^{d3}), \qquad (12)$$

where the upper subscripts $d1$, $d2$ and $d3$ indicate the selected types of defects. The analysis of various mother wavelets has shown that the optimal mother wavelet for the analyzed ultrasonic echo signals according to the criterion (Eq. 12) is the "Symlet-8". According to this conclusion we have reconstructed the analyzed signals $s_e(x_i,t)$ (Eq. 4) from the level 5 wavelet coefficients:

$$s_r(x_i,n) = \sum_{j=5}\sum_{k} \gamma_{j,k}(x_i)\psi_{j,k}(x_i,n). \qquad (13)$$

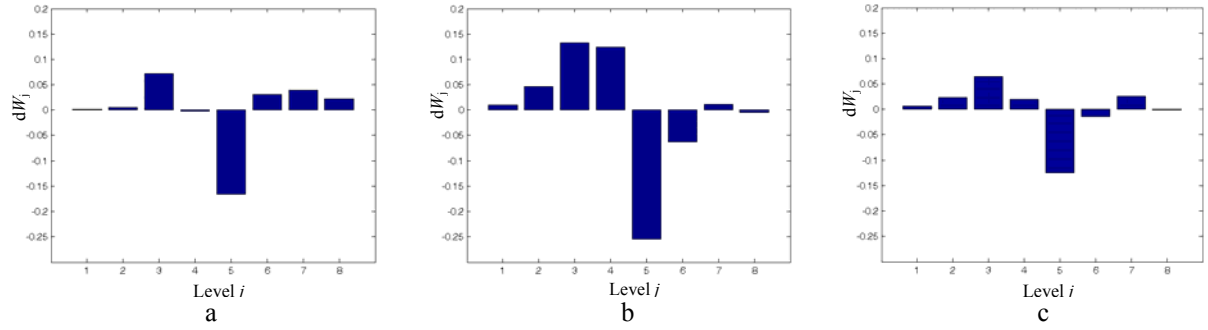

Fig.8. **The difference ΔW_j between the weighting coefficients W_{jav} and W^d_{jav} calculated by the "Coiflet-5" wavelet of the signals reflected by artificial defects SDH No.1 (a), No.2 (b) and No.3 (c).**

The *B-scans* with different artificial defects SDH No.1-3 obtained after the optimised wavelet transform are shown in Fig. 9. The presented results indicate significant improvement of the signals reflected by various defects (compare with Fig. 3d).

However from Fig. 9 follows that along the z axis precise measurements of the position and the size of the defect are not convenient due to the high frequency ripples caused by the radio frequency pulse signal. In order to solve this problem we propose to process additionally the signals $s_r(x_i, n)$ obtained after the DWT by the Hilbert transform in the time domain or along the z axis:

$$\tilde{s}(x_i,z) = \mathrm{H}\{s_r(x_i,n)\} = \frac{1}{\pi}\int_{-\infty}^{\infty}\frac{s_r(x_i,n)}{z-n}dn. \qquad (14)$$

The additionally processed *B-scans* after the Hilbert transform are presented in Fig. 10. In these *B-scans* all three artificial defects can be easily resolved and identified. After this step measurement of the defects coordinates and estimation of their size may be performed.

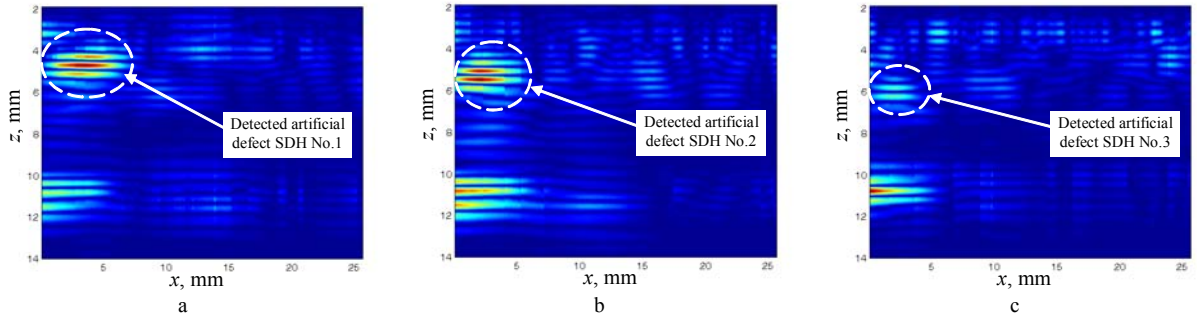

Fig. 9. ***B-scans* of the plastic pipe with the artificial defects along the coordinate x processed by the proposed method: a - SDH No.1; b - SDH No.2; c - SDH No.3.**

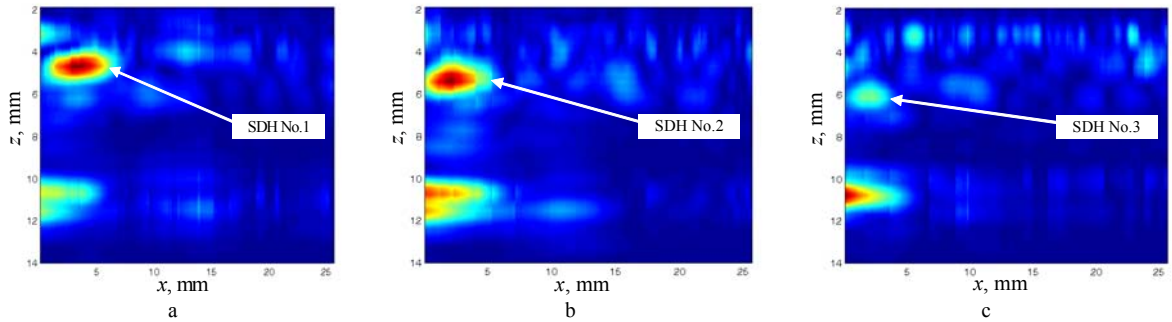

Fig.10. ***B-scans* of the pipe sample with the defects after the DWT additionally processed by the Hilbert transform: a - SDH No.1; b - SDH No.2; c - SDH No.3.**

4. Measurement of the defects location

Location of an artificial defect in the internal layer is described by the depth z_i and two coordinates x_i^1 and x_i^2, which correspond to the beginning and the end of the side drilled hole. Experimental estimation of the defect position was based on measurement of these coordinates in the B-scans, obtained after the Hilbert transform. The principle of measurement is explained in Fig. 11a-c. The first step is determination of the point (x_0, z_0) where the magnitude of the signal reflected by the defect is maximal, e.g. $x_0, z_0 = \max[s(x_i, z)]$ (Fig. 11a).

During the second step the defect length from the measured beginning and the end coordinates x_i^1 and x_i^2 of the defect was determined. These coordinates along the x-axis were estimated from the processed signal, normalized with respect to the maximal value at the point (x_0, z_0) (Fig.11b).

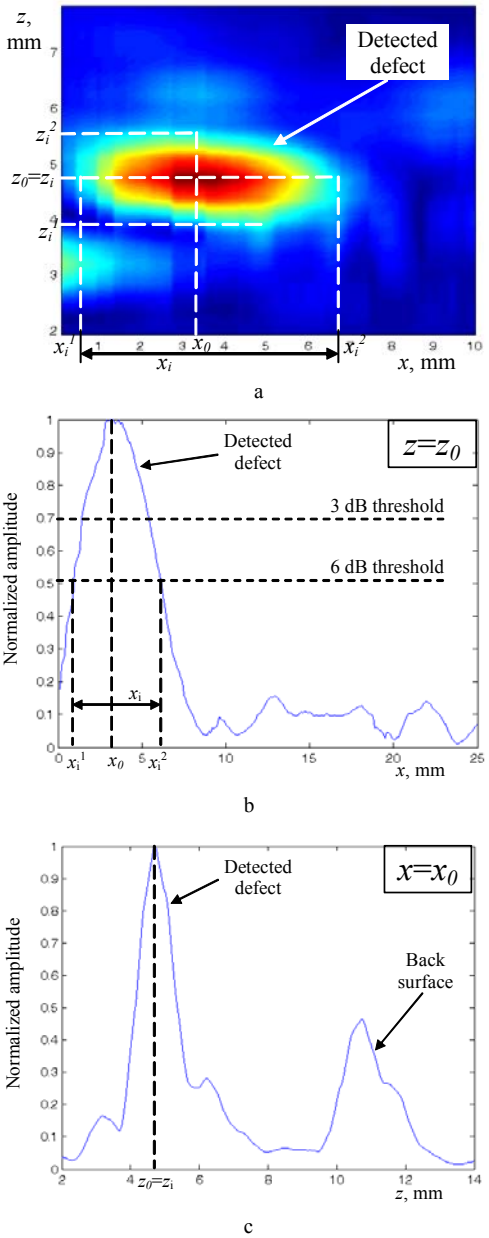

Fig.11. **Measurement of the coordinates x_i and z_0 of the side drilled hole in the processed *B-scans*.**

Table 1. **The results of measurements of the artificial defects**

Measured defect parameter	Measurement method	Defect SDH Nr.1.	Defect SDH Nr.2.	Defect SDH Nr.3.
Depth z_i, mm	Mechanical measurements	5.0	5.9	6.7
	Measured by the proposed algorithm	4.7	5.4	6.2
Error Δz_i, mm		0.3	0.5	0.5
Length x_i, mm	Mechanical measurements	6,3	5,1	4,4
	Measured by the proposed algorithm	5.3	4.6	3.6
Error Δx_i, mm		1.0	0.5	0.8

The coordinates x_i^1 and x_i^2 were found using 6dB threshold at $z=z_0$. The defect length is obtained as

$$x_l = x_i^2 - x_i^1 . \qquad (15)$$

The results of ultrasonic measurements of defects positions were compared with the results of the mechanical measurements carried out using the contact micrometer. Results of both measurements are presented in Table 1. Please note that in this table the absolute measurement errors Δz_i and Δx_i of the coordinate z and the defect length x_l are also given.

From the results presented follows that the absolute depth measurement errors obtained using the proposed algorithm do not exceed ±0.5 mm. The absolute measurements errors of the depth z_i for all artificial defects are very close. Measurement errors of the defect length are slightly bigger however doing not exceed ±1 mm. Please note that these results were obtained in the internal fibre-reinforced layer with a strong backscattered noise, caused by an internal structure of the pipe.

5. Conclusions

In this paper we present an ultrasonic signal processing algorithm for improved detection and location of defects in a three-layer polypropylene pipe with a fibreglass reinforced internal layer based on the discreet wavelet transform. This method consists of the improved algorithm eliminating the signals reflected by interfaces of the pipe layers, the optimized mother wavelet analysis and manipulation by the wavelet coefficients. The elimination of the reflected signals by interfaces is based on subtracting from each analysed signal the reference signal. Further the processed signal is decomposed into a sum of elementary wavelets. The optimal mother wavelet is chosen according to the introduced weighting coefficients and results of investigations of echo signals, reflected by different artificial defects in a multi-layer plastic pipe.

The experimental investigations have shown that after choosing the optimised mother wavelet “Symlet-8”, rejecting unwanted reflected signals and applying reconstruction of the useful signal according to the 5-th level coefficients, in the inhomogeneous layer detection of the artificial defect with the diameter 0.7 mm was obtained. The absolute measurement error of the defects location does not exceed ±1.0 mm.

References

1. Ultrasonic Testing. The nondestructive testing handbook, second edition. Birks A. S., Green R. E., Mclntire P. American Society for Nondestructive Testing. 1991. Vol. 7. P.893.
2. Nondestructive evaluation and quality control. ASM Handbook. ASM International. USA. 1994. Vol. 17. P. 795.
3. **Diederichs R.** New advantages for quality control of pPlastic gas pipes with an ultrasonic flaw detection rotation machine. NDTnet, May 1996. Vol.1. No.5. http://www.ndt.net/article/p_rot/p_rot.htm.
4. **Zeroug S.** Analytical modeling for fast simulations of ultrasonic measurements on fluid-loaded layered elastic structures. IEEE Transactions on Ultrasonics, Ferroelectrics and Frequency Control. May 2000. Vol. 47. No.3. P.565-574.
5. **Radko V. P., Troitskij V. A.** Detection and localizing of defects in welded joints of items from plastic using ultrasound. 15th World Conference on Nondestructive Testing, Roma (Italy) 15-21 October 2000. http://www.ndt.net/article/wcndt00/papers/idn487/idn487.htm.
6. **Honarvar F., Sheikhzadeh H., Moles M., Sinclair A. N.** Improving the time-resolution and signal-to-noise ratio of ultrasonic NDE signals. Ultrasonics. 2004. Vol. 41. P.755-763.
7. **Zhu Y., Weight J. P.** Ultrasonic non-destructive evaluation of highly scattering materials using adaptive filtering and detection. IEEE Transactions on Ultrasonics, Ferroelectrics and Frequency Control. 1994. Vol. 41. No.1. P.26-33.
8. **Izguierdo M. A. G., Hernadez M. G., Anaya J. J., Martinez O.** Speckle reduction by energy time-frequency filtering. Ultrasonics. 2004. Vol. 42. P.843-846.
9. **Gil Pita R., Vicen R., Rosa M., Jarabo M. P., Vera P., Curpian J.** Ultrasonic flaw detection using radial basis function network (RBFNs). Ultrasonics. 2004. Vol. 42. P.361-365.
10. **Croce R., Calmon P., Paradis L.** Modelling of propagation and echo formation in a multilayered structure. Ultrasonics. 2000. Vol.38. P.537-541.
11. **Chen X., Liu Y.** Multiple-cell modelling of fiber-reinforced composites with the presence of interfaces using the boundary element method. Computational Materials Science. 2001. Vol.21. P.86-94.
12. **Eriksson A. S., Mattsson J., Niklasson A. J.** Modelling of ultrasonic crack detection in anisotropic materials. NDT&E International. 2000. V ol.33. P.441-451.
13. **D'Orazio T., Leo M., Distante A., Guaragnella C., Pianese V., Cavaccini G.** Automatic ultrasonic inspection for internal defect detection in composite materials. NDT&E International. 2008. Vol.41. P.145-154.
14. **Liu S., Guo E., Levin V. M., Liu F., Petroyuk Yu. S., Zhang Q.** Application of pulse acoustic microscopy technique for 3D imaging bulk microstructure of carbon fiber-reinforced composites. Ultrasonics. 2006. Vol.44. P.1037-1044.
15. **Raišutis R., Kažys R., Mažeika L.** Application of the ultrasonic characterization methods highly attenuating plastic materials. NDT&E International. 2007. Vol.40. P.324-332.
16. **Kažys R., Pagodinas D., Tumšys O.** Detection of defects in multi-layered plastic cylindrical structures by ultrasonic method. Ultragarsas (Ultrasound), Kaunas: Technologija. 2002. Nr.2(43). P.7-12.
17. **Tian Q, Bilgutay N. M.** Statistical analysis of split spectrum processing for multiple target detection. IEEE Transactions on Ultrasonics, Ferroelectrics and Frequency Control. January 1998. Vol.45. No.1. P.251-256.
18. **Drai R., Khelil M., Benchaala A.** Flaw detection in ultrasonics using wavelet transform and split spectrum Processing. 15th World Conference on Nondestructive Testing, Roma (Italy) 15-21 October 2000. http://www.ndt.net/article/wcndt00/papers/idn589/idn589.htm.
19. **Rodriguez M. A., San Emeterio J. L., Lazaro J. C., Ramos A.** Ultrasonic flaw detection in NDE of highly scattering materials using wavelet transform and Wigner-Ville transform processing. Ultrasonics. 2004. Vol.42. P.847-851.
20. **Abbate A., Koay J., Frankel J., Schroder S. C., Das P.** Signal detection and noise suppression using a wavelet transform signal processor: Application to ultrasonic flaw detection. IEEE Transactions on Ultrasonics, Ferroelectrics and Frequency Control. January, 1997. Vol.44. No.1. P.14-26.
21. **Donoho D. L.** Non-linear wavelet methods for recovery of signals, densities, and spectra from indirect and noisy data. Proc. of Symphosia in Applied Mathematics. 1993. P.173-205.
22. **Daubechies I.** Ten lectures on wavelets. CBMS-NSF Lecture Notes Nr. 61, SIAM, 1992.
23. **Polikar R.** The wavelet tutorial. Part IV. Multiresolution analysis: the discrete wavelet transform. http://www.public.iastate.edu/~rpolikar/WAVELETS/
24. **Mallat S.** A theory for multiresolution signal decomposition: The wavelet representation. IEEE Trans. Patt. Anal. Machine Intell. 1989. Vol.11. No.7. P.674-693.
25. **Lazaro J. C., San Emeterio J. L., Ramos A., Fernadez-Marron J. L.** Influence of thresholding procedures in ultrasonic grain noise reduction using wavelets. Ultrasonics. 2002. Vol.40. P.263-267.
26. **Jonstone I. M., Silverman B. W.** Wavelet threshold estimators for data with correlated noise. J. Royal Statist. Soc. 1997. B59. P.319-351.
27. **Kažys R., Pagodinas D., Tumšys O.** Ultrasonic method for detection and location of defects in three-layer plastic pipe based on the wavelet transform. Ultragarsas (Ultrasound). Kaunas: Technologija. 2005. Nr.1 (54). P.33-38.
28. **Kamala G., Hashemi J., Barhorst A. A.** Discrete-wavelet analysis of acoustic emissions during fatigue loading of carbon fiber reinforced composites. Journal of Reinforced Plastics and Composites. 2001. Vol.20. P.222-238.

R. Kažys, O. Tumšys, D. Pagodinas

Naujas ultragarsinis metodas trijų sluoksnių plastikinio vamzdžio su sustiprintu vidiniu sluoksniu defektams aptikti

Reziumė

Daugiasluoksnių pluoštinių kompozicinių medžiagų ultragarsiniai neardomieji bandymai susiję specifinėmis problemomis, sąlygojamomis šių medžiagų dideliu akustiniu slopinimu ir aukštu struktūrinių triukšmų lygiu. Šie struktūriniai triukšmai atsiranda dėl ultragarso bangų išsklaidymo nuo sluoksnių nehomogeniškumo ir daugkartinių atspindžių tiriamosios medžiagos skirtingos kompleksinės akustinės varžos sluoksniuose.

Straipsnyje pateiktų tyrimų tikslas – sukurti naują ultragarsinių signalų apdorojimo metodą pluoštu sustiprinto trisluoksnio plastikinio vamzdžio vidiniams defektams aptikti. Pasiūlytame signalų apdorojimo algoritme panaudota ultragarsinių signalų, atsispindėjusių nuo vamzdžio sluoksnių paviršių, eliminavimo procedūra ir tolesnis skaitmeninis šių signalų apdorojimas bangelių transformacijos metodu. Atsispindėję nuo vamzdžio sluoksnių paviršių signalai eliminuojami atimant iš tiriamojo signalo pamatinį ultragarsinį signalą, suformuotą vamzdžio zonoje be defekto. Toliau signalas išskaidomas į elementarių bangelių sumą. Optimali pagrindinė bangelė nustatoma naudojant pasiūlytą naują įtakos koeficientų naudojimo metodiką ir atsižvelgiant į aido signalų, atsispindėjusių nuo įvairių dirbtinių defektų trisluoksniame vamzdyje, tyrimų rezultatus.

Pateikta spaudai 2008 09 04

DOI: 10.5755/j01.u.63.3.17074